A W-Band Electron Spin Echo Envelope Modulation Study of a Single Crystal of Azurin

J. W. A. Coremans,[†] O. G. Poluektov,[†] E. J. J. Groenen,*,[†] G. W. Canters,[‡] H. Nar,[§] and A. Messerschmidt[§]

Contribution from the Centre for the Study of Excited States of Molecules, Huygens Laboratory, Leiden University, P.O. Box 9504, 2300 RA Leiden, The Netherlands, Gorlaeus Laboratories, Leiden Institute of Chemistry, P.O. Box 9502, 2300 RA Leiden, The Netherlands, and Max Planck Institut für Biochemie, Martinsried bei München, Germany

Received November 5, 1996[⊗]

Abstract: At 95 GHz, deep electron spin echo envelope modulations of a single crystal of the blue copper protein azurin have been observed. The modulations arise from the *coordinated* nitrogens of the histidines that ligate to copper. From the ESEEM frequencies, hyperfine and quadrupole tensors of these nitrogens have been deduced. The isotropic hyperfine coupling of the copper-bound nitrogen of histidine-117 is 1.4 times larger than that of histidine-46. The anisotropic hyperfine tensors show that the wave function of the unpaired electron on both coordinated nitrogens mainly concerns the σ bonds with copper.

I. Introduction

The metal site of the blue copper protein azurin comprises a copper ion strongly bound to two histidines and a cysteine.[1,2] In the oxidized form of the protein, the copper has formal valence II which renders the site paramagnetic and amenable to electron paramagnetic resonance (EPR). In the pulsed version of this technique, electron spin echo (ESE) spectroscopy,[3] an electron spin resonance shows up as an echo following microwave excitation pulses. The hyperfine interaction of the electron spin with nuclear spins (e.g., those of the histidine nitrogens of azurin) may induce a variation of the echo intensity with the time between the microwave pulses which is known as electron spin echo envelope modulation (ESEEM).[4,5] If the hyperfine interaction is large enough compared with the nuclear Zeeman interaction (i.e., if M_I is not a good quantum number) microwaves may connect a nuclear sublevel of one electron spin manifold to two or more nuclear sublevels of the other electron spin manifold. Forbidden transitions become allowed, and if the excitation band width of the microwaves permits, a superposition of states is created whose time development will lead to modulations of the echo intensity with frequencies corresponding to the nuclear-sublevel separations.[3−5]

The occurrence of modulations critically depends on the relative magnitude of the external magnetic field and the internal field that the nuclear spin experiences. For blue copper proteins and model copper−imidazole complexes, it is found that at standard X-band (9 GHz) EPR frequencies the so-called remote nitrogens of the ligated histidines or imidazoles give rise to ESEEM signals (i.e., the nitrogens that are not bound to copper).[6] Such nitrogens have small hyperfine couplings,

typically 1 to 2 MHz,[7] and the (near) cancelation of Zeeman and hyperfine interaction in one electron spin manifold leads to particularly deep modulations.[8] These ESEEM studies have been used to identify histidine ligation in copper proteins[9] and to investigate hyperfine and quadrupole interaction of remote nitrogens.[10−13] However, ESEEM investigations at X-band frequencies do not provide information on the copper-bound nitrogens.

In recent years, the trend in EPR toward higher frequencies bears more and more fruit. For blue copper proteins, a spectrometer operating at W-band frequency (95 GHz) allowed us to perform pulsed EPR and electron nuclear double resonance (ENDOR) studies of submillimeter crystals of azurin and its mutant Met121Gln.[14−16] These studies benefited from the superior sensitivity and resolution of the ESE technique at W-band. In principle, a third advantage of the high frequency might be that other nuclei, silent at low frequencies, show up in ESEEM spectroscopy. However, frequencies and fields may easily become too high because modulations will no longer be seen when the Zeeman term becomes dominant in the nuclear Hamiltonian. Indeed, variation of the microwave frequency between 4 and 18 GHz has been successfully applied in ESEEM studies[17] but only recently weak modulations have been reported

---

[†] Huygens Laboratory.
[‡] Leiden Institute of Chemistry.
[§] Max Planck Institut für Biochemie.
[⊗] Abstract published in *Advance ACS Abstracts,* April 15, 1997.
(1) Baker, E. N. *J. Mol. Biol.* **1988,** *203,* 1071−1095.
(2) Nar, H.; Messerschmidt, A.; Huber, R.; van de Kamp, M.; Canters, G. W. *J. Mol. Biol.* **1991,** *221,* 765−772.
(3) *Pulsed EPR: A New Field of Applications*; Keijzers, C. P., Reijerse, E. J., Schmidt, J., Eds.; North-Holland: Amsterdam, 1989; pp 15−42.
(4) Mims, W. B. *Phys. Rev. B* **1972,** *5,* 2409−2419.
(5) Mims, W. B. *Phys. Rev. B* **1972,** *6,* 3543−3545.
(6) Mondovi, B.; Graziani, M. T.; Mims, W. B.; Oltzik, R.; Peisach, J. *Biochemistry* **1977,** *16,* 4198−4201.

(7) Jiang, F.; Karlin, K. D.; Peisach, J. *Inorg. Chem.* **1993,** *32,* 2576−2582.
(8) Flanagan, H. L.; Singel, D. J. *J. Chem. Phys.* **1987,** *87,* 5606−5616.
(9) Peisach, J. In *Bioinorganic chemistry of copper*; Karlin, K. D., Tyeklar, Z. Eds.; Chapman & Hall: New York, 1993; pp 21−33.
(10) Gerfen, G. J.; Singel, D. J. *J. Chem. Phys.* **1994,** *100,* 4127−4137.
(11) Goldfarb, D.; Fauth, J. M.; Farver, O.; Pecht, I. *Appl. Magn. Reson.* **1992,** *3,* 333−351.
(12) Jiang, F.; McCracken, J.; Peisach, J. *J. Am. Chem. Soc.* **1990,** *112,* 9035−9044.
(13) Dikanov, S. A.; Spoyalov, A. P.; Hüttermann, J. *J. Chem. Phys.* **1994,** *100,* 7973−7983.
(14) Coremans, J. W. A.; Poluektov, O. G.; Groenen, E. J. J.; Canters, G. W.; Nar, H.; Messerschmidt, A. *J. Am. Chem. Soc.* **1994,** *116,* 3097−3101.
(15) Coremans, J. W. A.; Poluektov, O. G.; Groenen, E. J. J.; Canters, G. W.; Nar, H.; Messerschmidt, A. *J. Am. Chem. Soc.* **1996,** *118,* 12141−12153.
(16) Coremans, J. W. A.; Poluektov, O. G.; Groenen, E. J. J.; Canters, G. W.; Warmerdam, G. C. M.; Nar, H.; Messerschmidt, A. *J. Phys. Chem.* **1996,** *100,* 19706−19713.
(17) Cosgrove Larsen, S.; Singel, D. J. *J. Phys. Chem.* **1992,** *96,* 9007−9013.

at 95 GHz[18] and even at 140 GHz.[19] For azurin, Q-band (35 GHz) ENDOR experiments have shown that the isotropic hyperfine interaction of the copper-bound nitrogens (Nδ) is 17 and 27 MHz, which is about 20 times that of the remote nitrogens.[15] As the Zeeman interaction scales up by an order of magnitude going from X- to W-band and echo modulations from the remote nitrogens are considerable at X-band, one might expect to see echo modulations from the coordinated nitrogens at W-band which would bring full hyperfine and quadrupole tensors of these nitrogens within reach.

Here, we report a W-band ESEEM study of a single crystal of azurin. A full orientational study has been performed and deep modulations have been observed. The modulations arise from the coordinated nitrogens of the ligating histidines and constitute the first modulations observed for these nitrogens in a copper protein. From the ESEEM frequencies, hyperfine and quadrupole tensors for both coordinated nitrogens are deduced and the principal axes of the quadrupole and hyperfine tensors corresponding to the absolute largest principal value are found to point approximately toward copper. The isotropic hyperfine interaction of the coordinated nitrogen of histidine-117 is found to be 1.4 times larger than that of histidine-46. The anisotropy of the hyperfine tensors is rationalized in terms of the dominating contribution of spin density in the Cu−Nδ σ bond to the anisotropic hyperfine tensor.

II. Experimental Section

The isolation and purification of azurin from *Pseudomonas aeruginosa* has been described elsewhere.[20] The single crystal of the oxidized protein was grown by vapor diffusion[2] and was kept in mother liquor containing 4.0 M ammonium sulfate, 0.7 M lithium nitrate, and 0.1 M acetate at pH 5.5. The dimensions of the crystal were submillimeter ($0.8 \times 0.4 \times 0.3$ mm^3). The space group of the crystal is $P2_12_12_1$, corresponding to orthorhombic symmetry. The unit cell with dimensions of $a = 57.8$, $b = 81.0$, and $c = 110.0$ Å contains 16 molecules with four molecules per asymmetric unit.

The ESEEM experiments were performed with the home-built W-band ESE spectrometer at a microwave frequency of 95 GHz and a temperature of 1.2 K. A detailed description of the pulsed EPR setup has been published.[21] The crystal was placed in a quartz tube and subsequently mounted into a cylindrical cavity. Both two- and three-pulse sequences were used in the ESEEM experiments. Microwave pulses of about 130 ns were used, and the repetition rate was 99 Hz. In the two-pulse experiments, the height of the echo was monitored as a function of the separation time τ between two microwave pulses, starting typically at 300 ns and increasing in 200 steps of 20 ns. In the three-pulse experiments, the time τ between the first two microwave pulses was kept fixed, typically at 350 ns. The height of the echo is monitored as a function of the separation time T between the last two microwave pulses, starting typically at 950 ns and successively increasing T in 350 steps of 20 ns. The echo decay underlying the modulations was approximated by a smooth function and subtracted from the time−domain data prior to Fourier transformation.

The crystal as mounted in the sample tube in the cavity had an arbitrary orientation with respect to the laboratory frame. The directions of the crystallographic axes (a, b, and c) were determined with respect to the laboratory frame through EPR with high accuracy (∼2°). In the EPR study of a single crystal of azurin from *Ps. aeruginosa*, the directions of the principal axes (x, y, and z) of the **g**-tensor of all 16 molecules in the unit cell were established with respect to a, b, and c.[14] These data have been used in the present ESEEM study to obtain

(18) Prisner, T.; Rohrer, M.; Möbius, K. *Appl. Magn. Reson.* **1994**, *7*, 167.

(19) Becerra, L. R.; Gerfen, G. J.; Bellew, B. F.; Bryant, J. A.; Hall, D. A.; Inati, S. J.; Weber, R. T.; Un, S.; Prisner, T.; McDermott, A. E.; Fishbein, K. W.; Kreischer, K. E.; Temkin, R. J.; Singel, D. J.; Griffin, R. G. *J. Magn. Reson. A* **1995**, *117*, 28−40.

(20) van de Kamp, M.; Hali, F. C.; Rosato, N.; Finazzi Agro, A.; Canters, G. W. *Biochim. Biophys. Acta* **1990**, *1019*, 283−292.

(21) Disselhorst, J. A. J. M.; van der Meer, H.; Poluektov, O. G.; Schmidt, J. *J. Magn. Reson. A* **1995**, *115*, 183−188.
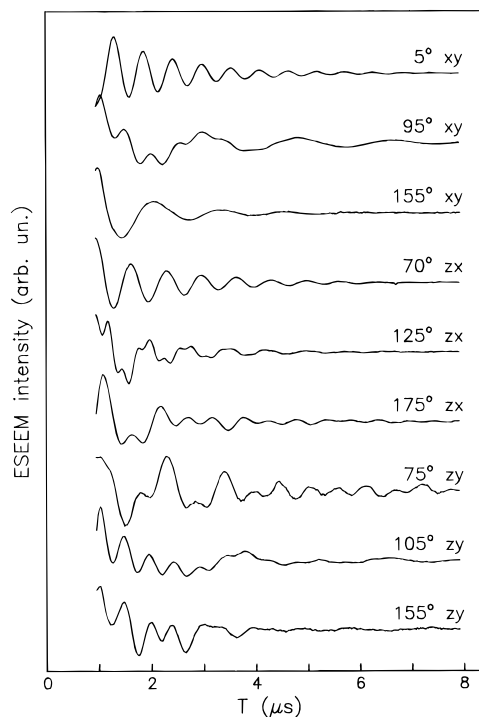

Figure 1. Three-pulse electron spin echo envelope modulations for a single crystal of azurin. Data for nine different orientations of the magnetic field with respect to the **g**-tensor principal axes system (x, y, z) are shown. The decay of the echo intensity has been removed to emphasize the different frequencies present in the modulation pattern for different orientations of the magnetic field. The value of τ was 350 ns.

the directions of x, y, and z of one molecule in the unit cell in the laboratory frame. All ESEEM experiments were performed with respect to the x, y, and z axes of that molecule. Note that, previously, the EPR data were combined with X-ray data yielding the orientation of the x, y, and z axes in the copper site, and consequently, directions defined with respect to xyz can be translated into directions with respect to the copper site and vice versa.

III. Results

Considerable modulations of the electron spin echo intensity have been observed for a single crystal of azurin at 95 GHz. Examples of modulation patterns observed in the three-pulse experiments for various orientations of the magnetic field $\vec{B}_0$ with respect to the crystal are given in Figure 1. All time profiles belong to one of the 16 molecules in the unit cell and at each orientation the strength of $\vec{B}_0$ was chosen such as to be in resonance with the EPR transition of that molecule. The x, y, and z axes of the **g**-tensor of that molecule serve as the reference frame. For instance for the top spectrum in Figure 1, $\vec{B}_0$ was oriented in the xy plane of the **g**-tensor and rotated 5° from the x axis toward the y axis. As can be seen from Figure 1, the modulation pattern clearly varies with the orientation of $\vec{B}_0$. The frequencies present in the modulation patterns are derived by Fourier transformation and summarized in Figure 2. Not only the frequencies depend on the orientation of $\vec{B}_0$, but also the depth and the duration of the modulations. Modulation depths up to 20% of the total echo intensity and modulations lasting for more than 8 μs have been observed. For some orientations of $\vec{B}_0$, the modulations were shallow and/or lasted shortly. For instance, between 60° and 90° in the xy plane, the modulations were not very pronounced. The corresponding FFT spectrum contained intensity below 1 MHz but individual frequencies could not be accurately determined. For orientations of $\vec{B}_0$ within approximately 40° of the z and −z axes in the zy plane and especially in the zx plane, the
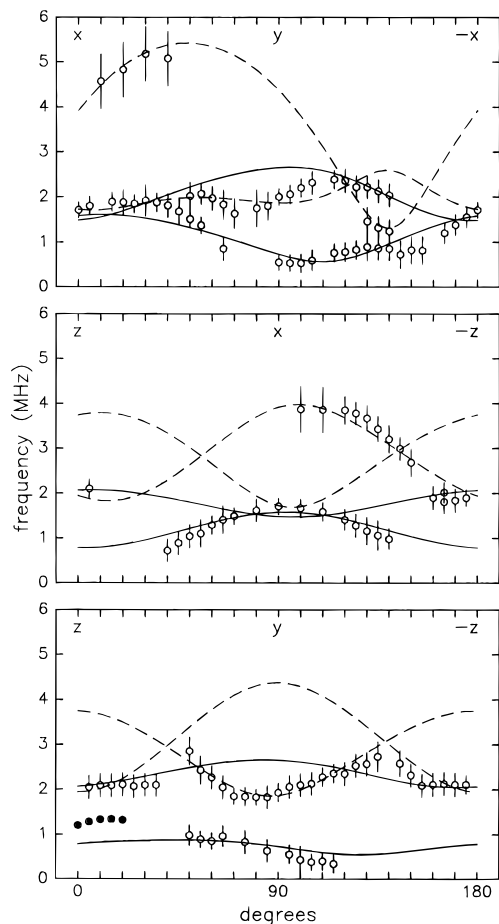
Figure 2. The ESEEM frequencies of the coordinated nitrogens as a function of the direction of the magnetic field in the *xy*, *zx*, and *zy* principal planes of the **g**-tensor. The circles represent the experimental frequencies, the crosslines indicate the line width, and the curves represent fits based on eq 1. The solid curves correspond to the coordinated nitrogen of histidine-46 and the dashed ones to that of histidine-117. All frequencies have been obtained from three-pulse experiments except the highest frequencies from 10° to 40° *xy* and 100° to 110° *zx* that were obtained from two-pulse experiments. The frequencies below 1.5 MHz for orientations of the magnetic field near the *z* axis in the *zy* plane are represented by filled circles (see text).

frequencies below 1.5 MHz were not well resolved and are therefore omitted in Figure 2. For orientations of $\vec{B}_0$ between 0° and 20° in the *zy* plane some low frequencies have been determined and are represented in Figure 2 as filled circles. These frequencies have to be treated with caution because the corresponding bands are superimposed on a broad signal in the low-frequency region of the spectrum. In addition, it did not become clear how these frequencies have to be connected with frequencies observed for $\vec{B}_0$ near the *z* and −*z* axes in the *zx* plane. These complications may well result from the overlap of EPR transitions of different molecules in the unit cell for orientations of $\vec{B}_0$ near the *z* axis.[14] In the ENDOR study of a single crystal of azurin,[15] the overlap of EPR transitions resulted in broadening of the ENDOR lines.

Also, two-pulse experiments have been performed while the orientation of $\vec{B}_0$ was systematically varied in the three principal planes of the **g**-tensor. Examples of time profiles obtained for different orientations of $\vec{B}_0$ are given in Figure 3. Modulations, sometimes reaching a depth of 25% of the echo intensity, are visible superimposed on a fast decay. For some orientations of $\vec{B}_0$ shallow modulations were observed. This happened roughly speaking for the same orientations of $\vec{B}_0$ as in the three-pulse experiment. The higher frequencies in the two-pulse experiment reproduce those from the three-pulse experiment
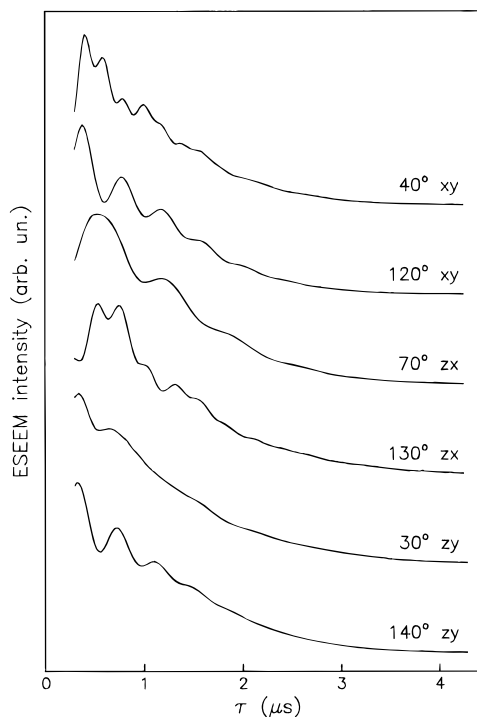

Figure 3. Two-pulse electron spin echo envelope modulations for a single crystal of azurin. Data for six different orientations of the magnetic field with respect to the **g**-tensor principal axes system (*x*, *y*, *z*) are shown.
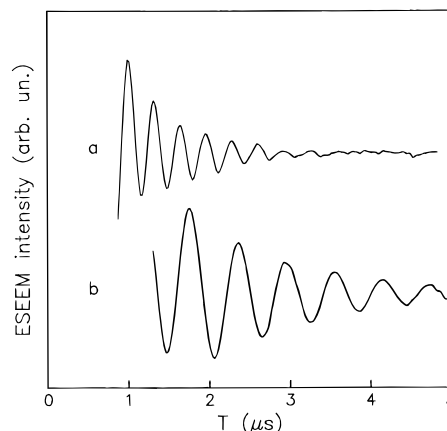

Figure 4. Three-pulse ESEEM time−domain data for a single crystal of ^{15}N azurin (a) and ^{14}N azurin (b). The orientation of the magnetic field with respect to the **g**-tensor principal axes system was identical in both experiments (100° *zx*).

while the frequencies below 1 MHz were determined more accurately in the three-pulse experiment. Additional frequencies were observed above 3.5 MHz for orientations of $\vec{B}_0$ between 10° and 40° *xy* and between 100° and 110° *zx*. These frequencies are included in Figure 2.

For a single crystal of ^{15}N-labeled azurin, preliminary three-pulse ESEEM experiments were performed. Never more than one frequency was observed in the modulations for different orientations of $\vec{B}_0$. In Figure 4, the modulation pattern of a crystal of ^{15}N azurin is compared with that of a crystal of ^{14}N azurin at identical orientations of $\vec{B}_0$ with respect to *xyz*. Both modulations reveal a single frequency, 1.62 MHz for ^{14}N azurin and 3.15 MHz for ^{15}N azurin.

IV. Data Analysis

The ESE envelope modulations observed for a single crystal of azurin at W-band arise from the coupling of the unpaired

electron spin with the nuclear spin of the coordinated nitrogens of the copper-ligating histidines. Only nitrogens qualify because the modulation patterns clearly change upon substitution of ^{15}N for ^{14}N. As exemplified in Figure 4, distinctly different frequencies have been found for single crystals of ^{14}N and ^{15}N azurin for identical orientations of $\vec{B}_0$. The origin of this change lies in the fact that ^{14}N has nuclear spin $I = 1$ and nuclear g-factor $g(^{14}$N$) = 0.4037$ while ^{15}N has nuclear spin $I = \frac{1}{2}$ and nuclear g-factor $g(^{15}$N$) = -0.5664$.

Closer examination reveals that the modulations must arise from the coordinated nitrogens. In general, modulations occur because microwave excitation results in a coherent superposition of nuclear spin states (i.e., the microwaves couple a nuclear spin level in one electron spin manifold to more than one nuclear spin level in the other electron spin manifold). For this to happen, forbidden transitions have to become partially allowed and the splitting of the nuclear spin levels in (one of) the electron spin manifolds has to be smaller than the excitation band width. At W-band the nuclear Zeeman frequency of ^{14}N is about 10 MHz. Forbidden transitions become allowed when the hyperfine interaction divided by $2h$ is on the order of the nuclear Zeeman frequency. If equal, the hyperfine interaction fulfils the so-called "exact-cancelation" condition[8] (i.e., in one of the electron spin manifolds the splitting of the nuclear spin levels owing to the nuclear Zeeman interaction is canceled by the hyperfine interaction, a situation that leads to deep modulations). For azurin, the nitrogens with a hyperfine interaction closest to the cancelation condition are the coordinated nitrogens of the copper-ligating histidines. Isotropic hyperfine interactions of 17 and 27 MHz have been found from Q-band ENDOR experiments on frozen solutions.[22]

The spin Hamiltonian describing the system of the unpaired electron spin ($S = \frac{1}{2}$) and the ^{14}N nuclei can be divided in an electronic and a nuclear part since the electron Zeeman term at W-band is much larger than the hyperfine interaction. The nuclear Hamiltonian includes a Zeeman, a hyperfine, and a quadrupole interaction term for each nitrogen

$$\mathcal{H}_n = -\mathbf{g}(^{14}\text{N})\beta_n \vec{I}\cdot\vec{B}_0 + \langle\vec{S}\rangle\cdot\vec{\vec{A}}\cdot\vec{I} + \vec{I}\cdot\vec{\vec{Q}}\cdot\vec{I} \qquad (1)$$

Here, β_n is the nuclear Bohr magneton, $\langle\vec{S}\rangle$ the expectation value of the electron spin angular-momentum operator $\vec{S}$, $\vec{\vec{A}}$ the hyperfine tensor, and $\vec{\vec{Q}}$ the quadrupole tensor. For the coordinated nitrogens only frequencies from the "canceled" manifold can be detected at W-band since the energy difference between the nuclear spin levels in the other manifold is much too large. Each nitrogen gives rise to at most three frequencies in the modulation pattern, one of these corresponds to the so-called $\Delta M_I = 2$ transition. As can be seen from Figure 2, no more than three frequencies have been observed in the ESEEM experiments. However, if the ESEEM frequencies would arise from a single nucleus, the two lowest frequencies should add up to the highest, and this is not the case. Both coordinated nitrogens contribute to the modulation pattern, and in principle, also combination frequencies of the fundamental frequencies of the two nitrogens can be observed.

To gain insight into which frequencies in Figure 2 have to be assigned to histidine-46 and which to histidine-117, simulations based on the Hamiltonian of eq 1 were performed. In the simulation, each coordinated nitrogen is described by 11 parameters. The quadrupole tensor is described by five parameters, three to define the orientation of the principal axes x', y', and z' with respect to the **g**-tensor principal axes system, and e^2qQ and η to represent the principal values of the

quadrupole tensor, since it is a traceless tensor. The hyperfine tensor is described by six parameters, three to define the orientation of the principal axes x'', y'', z'' with respect to the **g**-tensor principal axes system and three for the principal values $A_{x''x''}$, $A_{y''y''}$ and $A_{z''z''}$. In order to describe the principal axes of hyperfine and quadrupole tensors, a reference frame is defined for each coordinated nitrogen: one axis perpendicular to the plane of the histidine and one axis parallel to the bisector of the Cγ−Nδ and the Cϵ−Nδ bonds (for both coordinated nitrogens this axis makes an angle of 3° with the Cu−Nδ axis and we consider these two axes parallel in the rest of the discussion). In the first simulations, we took the principal axes of the quadrupole and hyperfine tensors of every coordinated nitrogen collinear and coincident with the reference frame: z' and z'' perpendicular to the plane of the histidine and x' and x'' parallel to the bisector of the Cγ−Nδ and the Cϵ−Nδ bonds. As far as the discussion of the quadrupole axes is concerned, this starting point is inspired by three observations: (1) in an ENDOR study of a single crystal of Cu(II)-doped L-histidine deuterochloride monodeuterohydrate, one quadrupole axis of the coordinated nitrogen was found to make an angle of only 11° with z' and another of only 6° with x';[23] (2) in ab initio SCF studies of trimeric imidazole, which mimics the solid state, one of the principal axes of the quadrupole tensor for the Nδ was calculated to be perpendicular to the plane of the imidazole while another axis made an angle of 13° with the bisector;[24] (3) the quadrupole data for a number of coordinated imidazole complexes have been rationalized in a Townes−Dailey model using the principal axes system as described above.[25]

Simulations with isotropic hyperfine interactions of 17 and 27 MHz, corresponding to the values reported by Werst et al.,[22] revealed that the smallest isotropic hyperfine value had to be assigned to the coordinated nitrogen of histidine-46 and the largest one to that of histidine-117 in order to achieve qualitative agreement between experimental and calculated frequencies. The simulations showed that for most orientations the low frequencies had to be assigned to the coordinated nitrogen of histidine-46 (as the hyperfine interaction of this nitrogen is closest to cancelation) and the high ones to the coordinated nitrogen of histidine-117. In addition, the simulations indicated that the frequencies in Figure 2 correspond to fundamental frequencies of both nitrogens and not to combination frequencies or frequencies associated with $\Delta M_I = 2$ transitions.

Subsequently, the experimental frequencies belonging to each nucleus were successively analysed by nonlinear least-squares fits to the Hamiltonian of eq 1. The experimental data sets are limited and did not allow variation of all 11 parameters. Therefore, in the first instance, the directions of the principal axes of the hyperfine and quadrupole tensors were held along the reference frame (vide supra). With this restriction already a fair agreement between calculated and experimental frequencies was obtained for both coordinated nitrogens, albeit that the lowest frequencies in the xy plane were not reproduced. These frequencies belong to the coordinated nitrogen of histidine-46 and vary from 0.45 to 1.8 MHz when $\vec{B}_0$ is turned from the y axis to the x or $-x$ axis. This feature could be satisfactorily explained when the orientations of the principal axes x' and y' of the quadrupole tensor of histidine-46 were allowed to vary. In the final analysis, all of the experimental frequencies, represented by open circles in Figure 2, were included and only the directions of the principal axes of the hyperfine and

(22) Werst, M. M.; Davoust, C. E.; Hoffman, B. M. *J. Am. Chem. Soc.* **1991**, *113*, 1533−1538.

(23) McDowell, C. A.; Naito, A.; Sastry, D. L.; Cui, Y. U.; Sha, K.; Yu, S. X. *J. Mol. Struct.* **1989**, *195*, 361−381.

(24) Palmer, M. H.; Scott, F. E.; Smith, J. A. S. *Chem. Phys.* **1983**, *74*, 9−14.

(25) Ashby, C. I. H.; Cheng, C. P.; Brown, T. L. *J. Am. Chem. Soc.* **1978**, *100*, 6057−6063.

Table 1. Principal Values (in MHz) of the Hyperfine and Quadrupole Tensors of the Coordinated Nitrogens and Directions of the Principal Axes of the Hyperfine Tensor (x'', y'', and z'') with Respect to the Principal Axes of the **g**-Tensor[a]

	e^2qQ/h	η	$Q_{x'x'}/h$	$Q_{y'y'}/h$	$Q_{z'z'}/h$	a_{iso}/h	$A_{x''x''}/h$	$A_{y''y''}/h$	$A_{x''x''}/h$		x	y	z
Nδ (His46)	2.9	0.5	1.44	−1.08	−0.36	18.1	19.1	18.0	17.2	x''	−0.933	0.353	−0.068
			(0.3)	(0.3)	(0.3)	(0.4)	(0.3)	(0.4)	(0.4)	y''	−0.350	−0.851	0.392
										z''	0.081	0.389	0.918
Nδ (His117)	2.5	0.6	1.27	−0.25	−1.02	25.1	27.8	24.0	23.6	x''	0.572	0.819	0.051
			(0.4)	(0.4)	(0.4)	(0.3)	(0.4)	(0.3)	(0.3)	y''	0.654	−0.417	−0.632
										z''	−0.496	0.395	−0.774

[a] The x'', y'', and z'' axes system is collinear to the reference frame (see text).

quadrupole tensors perpendicular to the planes of the respective histidines (i.e., the z' and the z'' axes) were kept fixed. The calculated frequencies are indicated in Figure 2 by the solid and dashed lines for histidines-46 and -117, respectively. The results of these fits are given in Table 1. The inclusion of the orientations of the principal axes of the hyperfine and quadrupole tensors in the plane of the histidines as variables in the fits hardly affected the result for the hyperfine tensors. In doing so, the x'' and y'' axes rotate less than 10° with respect to the molecular frame and the variation of the principal values stays within the error margin. This holds as well for the quadrupole tensor of the coordinated nitrogen of histidine-117, but for histidine-46 the x' and y' axes rotate (right-handedly) 25° around the z' axis. For both coordinated nitrogens, the $A_{x''x''}$ was found to be the largest principal value of the hyperfine tensor and $A_{z''z''}$ the smallest. The absolute value of $Q_{x'x'}$ was the largest for both coordinated nitrogens, while $|Q_{y'y'}|$ was larger and smaller than $|Q_{z'z'}|$ for the coordinated nitrogens of histidine-46 and histidine-117, respectively.

The errors in Table 1 are the standard deviations from the fits of the experimental frequencies represented by the open circles in Figure 2. The ESEEM frequencies can only be partially followed over the three principal planes, and a small change in the number of frequencies included in the fits sometimes caused a larger variation of the parameters from the fits than implied by the standard deviation. The low frequencies in the zy plane near the z axis, indicated by the filled circles in Figure 2, most likely originate from the coordinated nitrogen of histidine-46. When these frequencies are included in the fits of the coordinated nitrogen of histidine-46, the overall agreement between experimental and calculated frequencies remains satisfactory, although the frequencies in the zx plane get less well described. The principal values of the hyperfine tensor, $A_{x''x''}$, $A_{y''y''}$, and $A_{z''z''}$, become 19.3, 17.3, and 16.8 MHz. Compared to the values in Table 1, $A_{y''y''}$ and $A_{z''z''}$ change considerably. The order of the principal values remains the same as that in Table 1 ($A_{x''x''} > A_{y''y''} > A_{x''x''}$), but the anisotropy of the hyperfine interaction (defined as $(|A_{x''x''}| - |A_{z''z''}|)/|a_{iso}|$) has increased from 11 to 14%. The quadrupole tensor hardly changes when these low frequencies near the z axis are included in the fit, albeit that the rotation of the principal axes in the plane with respect to the reference frame becomes somewhat smaller (20° instead of 25°). For the coordinated nitrogen of histidine-117, variation of the set of experimental frequencies included in the fits influences the principal values of the quadrupole tensor more than those of the hyperfine tensor. When the frequencies around 1.8 MHz near the x axis in the xy plane were excluded from the fits, the values of $Q_{y'y'}$ and $Q_{z'z'}$ varied by 0.5 MHz.

V. Discussion

Experiments have shown that at W-band the nitrogens of the histidine ligands which coordinate to the copper ion in azurin give rise to deep electron spin echo envelope modulations. On the other hand, it is well-known that the remote nitrogens of the histidines may be probed by ESEEM methods at lower (e.g.,

X-band frequencies). By going to higher microwave frequencies and higher magnetic fields, nuclei with larger hyperfine interactions are selected in the ESEEM experiment.

From the analysis of the ESEEM spectra, we have derived quadrupole and hyperfine tensors of the copper-coordinated nitrogen nuclei. First, we discuss the quadrupole tensors, and second, we discuss the hyperfine tensors.

The principal axes systems of the quadrupole tensors of both coordinated nitrogens are found to coincide more or less with the respective reference frames as defined in section IV. For histidine-117, the difference is not significant in view of the error margin of 10°. For histidine-46, the principal axes in the molecular plane make an angle of about 25° with the corresponding ones of the reference frame. It appears as if for the Nδ (coordinated or not) the principal axes of the quadrupole tensor are not as rigorously fixed to the molecular structure of the imidazole as for the remote nitrogens.[15] For Nδs, significant variations in the orientation of the principal axes of the quadrupole tensor have been reported in the literature,[23,24] while for Nεs such variations seem to be limited to 6°.[15,26−28] The values found for e^2qQ and η are in the range spanned by imidazole and a series of coordinated imidazole complexes (e^2qQ/h of 3.3−1.9 MHz, η of 0.1−0.7).[25] For the coordinated nitrogen of histidine-46 $|Q_{x'x'}|$ corresponds to the largest principal value and $|Q_{z'z'}|$ to the smallest. This order of the principal values is in accordance with that found for the coordinated nitrogen in Cu(II)-doped L-histidine deuterochloride monodeuterohydrate[23] and in trimeric imidazole[24] and follows the result of the Townes−Dailey analysis for a number of coordinated imidazole complexes.[25] For the coordinated nitrogen of histidine-117, the value of $|Q_{z'z'}|$ is larger than that of $|Q_{y'y'}|$. This remarkable observation seems to point to a slightly different relative occupation of the two imidazole (N−C) σ orbitals and the p$_\pi$ orbital compared with that for histidine-46. A value of $|Q_{z'z'}|$ larger than that of $|Q_{y'y'}|$ has also been inferred for the nitrogen of coordinated pyridine.[29]

The values of the isotropic hyperfine coupling of the Nδs turn out to be 18 and 25 MHz, comparable with the couplings of 17 and 27 MHz deduced from Q-band ENDOR experiments of frozen solutions of azurin previously.[22] The W-band ESEEM study on the azurin single crystal allows the definite assignment of the largest hyperfine coupling to the copper-coordinated nitrogen of histidine-117 and the smallest one to that of histidine-46. Their ratio of 1.4 is similar to that observed for the remote nitrogens of the histidines in azurin from the single-crystal ENDOR study[15] (i.e., the isotropic hyperfine interaction of the remote nitrogen of histidine-117 is 1.5 times larger than that of histidine-46). The present ESEEM data for the coordinated nitrogens nicely corroborate our earlier suggestion that the

(26) Colaneri, M. J.; Peisach, J. *J. Am. Chem. Soc.* **1995**, *117*, 6308−6315.

(27) McDowell, C. A.; Naito, A.; Sastry, D. L.; Takegoshi, K. *J. Magn. Reson.* **1986**, *69*, 283−292.

(28) Colaneri, M. J.; Peisach, J. *J. Am. Chem. Soc.* **1992**, *114*, 5335−5341.

(29) Hsieh, Y. N.; Rubenacker, G. V.; Cheng, C. P.; Brown, T. G. *J. Am. Chem. Soc.* **1977**, *99*, 1384−1389.

histidines carry a different total spin density while the spin density distribution in the ring is comparable.

As regards the anisotropic hyperfine tensors, the observed directions of the principal axes deviate less than 10° from those of the reference axes for both coordinated nitrogens. Because the difference is insignificant compared with the experimental error, we consider reference frame and hyperfine principal axes system to coincide.

The principal values of the anisotropic hyperfine tensors are 2.7, −1.1, and −1.6 MHz and 1.0, −0.1, and −0.9 MHz for histidines-117 and -46, respectively. The anisotropic hyperfine interaction is significantly larger for the nitrogen of histidine-117 than for that of histidine-46, as was the case for the isotropic hyperfine coupling. For both coordinated nitrogens, the positive and absolute largest principal value is associated with x'' (i.e., the axis oriented along the Cu−Nδ vector) and the smallest principal value with z'' (i.e., the principal axis perpendicular to the histidine ring). For the Nδ of histidine-117, the anisotropic hyperfine tensor is roughly axial with the unique axis (i.e., the axis associated with the positive and absolute largest principal value) along x''. This indicates that the spin density on Nδ is mainly in the σ bond with the copper ion. For spin density in a σ orbital toward copper, a tensor axial about x'' is expected, while for spin density in a p$_\pi$ orbital perpendicular to the imidazole plane, the tensor would have shown axiality about z''. The observation of a ground state σ interaction between copper and histidine nitrogen is in line with the result of an Xα-SCF-SW study on a model site of the blue copper protein plastocyanin[30] where it was found that the interaction between the copper and the coordinated nitrogens of the histidines is best described as σ overlap of the copper d$_{xy}$ orbital with the Nδ lone pair orbital (the axes system used for the copper orbitals is as follows: the x axis is parallel to the copper cysteine sulfur bond and the z axis is perpendicular to the NNS plane). For the coordinated nitrogen of histidine-46, the anisotropic hyperfine tensor is not that accurately determined, and yet the positive and absolutely largest principal value is associated with x'', which indicates that also for histidine-46 the wave function of the unpaired electron on the Nδ mainly has σ character. Inclusion of the low frequencies near z in the fits brings the anisotropic hyperfine tensor of the coordinated nitrogen of histidine-46 more in line with that of histidine-117. The tensor becomes more axial (1.5, −1.0, and −0.5 MHz), and the anisotropy gets comparable with that for histidine-117 (14% versus 16%). However, in view of the uncertainty with respect to these frequencies in the present ESEEM data the inclusion of the latter frequencies in the fit can not be substantiated. Simulations of the intensities of the ESEEM lines of the coordinated nitrogen of histidine-46 may be helpful to arrive at a more accurate anisotropic hyperfine tensor.

The anisotropy of the hyperfine interaction of the coordinated nitrogens of about 15% qualitatively agrees with the 10% anisotropy estimated from the Q-band ENDOR spectra of frozen solutions of azurin.[22] Also for the coordinated nitrogens of copper−imidazole complexes and a number of other copper proteins the anisotropy has been inferred to be small from ENDOR measurements at the high- and low-field edge of the EPR spectrum.[31,32]

As discussed above, the main contribution to the anisotropic

hyperfine tensor of the coordinated nitrogens arises from spin density in the σ orbital. To get a more quantitative insight in the anisotropic hyperfine tensor of the coordinated nitrogen of histidine-117, we apply a simple model. We consider three sp^2 hybrid atomic orbitals on the coordinated nitrogen, expressed in terms of 2s and 2p Slater orbitals. The sp^2 hybrid orbital that points toward copper should mimic the σ orbital. Therefore, in this case the effective nuclear charge of the Slater orbitals was more or less arbitrarily chosen to be 2.65 corresponding to an average distance of the electron from the coordinated nitrogen of 1 Å (i.e., half of the Cu−Nδ distance). For the two sp^2 hybrid orbitals in the ring, a standard value of the effective nuclear charge was used ($Z = 4.35$).[33] The anisotropic hyperfine interaction was calculated from these three sp^2 hybrid orbitals.[15] The spin density in the two sp^2 orbitals in the histidine ring was taken to be equal as the rotation of the principal axes in the plane of the histidine with respect to the reference frame was found to be negligible. The spin density of the unpaired electron in these two orbitals and in the σ bond is obtained from a linear least-squares fit of the experimental anisotropic hyperfine tensor. Most of the spin density, 17%, is found in the σ orbital. This results in an axial tensor with the positive and largest principal value associated with x''. In each of the two sp^2 orbitals in the histidine ring a spin density of 0.5% is found. The small spin density in these orbitals accounts for the non-axiality of the tensor. The total spin density in the three orbitals is 18%. This is reasonable in view of the spin density in the copper d$_{xy}$ orbital (this orbital contributes roughly 10% spin density to the σ orbital as estimated from the 41% spin density in the d$_{xy}$ orbital of plastocyanin[34]) and the spin density on the coordinated nitrogen (9%), as obtained from the analysis of the anisotropic hyperfine tensor of the remote nitrogen.[15,35] The model shows that most of the spin density on the coordinated nitrogen concerns the σ bond, and owing to its delocalized character, the anisotropy of the hyperfine interaction is relatively small.

In conclusion, we emphasize that the use of microwaves at much higher frequencies than X-band yields new possibilities for ESEEM spectroscopy. At W-band, the coordinated instead of the remote nitrogens of copper proteins can be studied. For azurin, the W-band ESEEM study of a single crystal resulted in hyperfine and quadrupole tensors for the coordinated nitrogens of histidines-46 and -117. The hyperfine tensors show that the wave function of the unpaired electron on the coordinated nitrogens mainly concerns the σ bonds with copper.

(30) Guckert, J. A.; Lowery, M. D.; Solomon, E. I. *J. Am. Chem. Soc.* **1995**, *117*, 2817−2844.
(31) Yokoi, H. *Biochem. Biophys. Res. Commun.* **1982**, *108*, 1278−1284.
(32) van Camp, H. L.; Sands, R. H.; Fee, J. A. *J. Chem. Phys.* **1981**, *75*, 2098−2107.

(33) Singel, D. J.; van der Poel, W. A. J. A.; Schmidt, J.; van der Waals, J. H.; de Beer, R. *J. Chem. Phys.* **1984**, *81*, 5453−5461.
(34) George, S. J.; Lowery, M. D.; Solomon, E. I.; Cramer, S. P. *J. Am. Chem. Soc.* **1993**, *115*, 2968−2969.
(35) In the analysis of the anisotropic hyperfine tensors of the remote nitrogens of histidines-46 and −117 that we have performed previously,[15] spin density on the Nδ atoms was found to contribute substantially to these tensors. In the analysis, the spin density on the Nδ atoms was distributed equally over the three sp^2 hybrid orbitals while the present ESEEM data show that most of the spin density is localized in the sp^2 hybrid orbital pointing toward copper. However, this difference does not essentially affect our conclusions drawn from the anisotropic hyperfine tensors of the remote nitrogens.